EUROPEAN ORGANIZATION FOR NUCLEAR RESEARCH (CERN)

Observation of the $B_s^0 \to \chi_{c1}(3872)\pi^+\pi^-$ decay

LHCb collaboration

Abstract

The first observation of the $B_s^0 \to (\chi_{c1}(3872) \to J/\psi\pi^+\pi^-)\,\pi^+\pi^-$ decay is reported using proton-proton collision data, corresponding to integrated luminosities of 1, 2 and $6\,\text{fb}^{-1}$, collected by the LHCb experiment at centre-of-mass energies of 7, 8 and 13 TeV, respectively. The ratio of branching fractions relative to the $B_s^0 \to (\psi(2S) \to J/\psi\pi^+\pi^-)\,\pi^+\pi^-$ decay is measured to be

$$\frac{\mathcal{B}\left(B_s^0 \to \chi_{c1}(3872)\pi^+\pi^-\right) \times \mathcal{B}\left(\chi_{c1}(3872) \to J/\psi\pi^+\pi^-\right)}{\mathcal{B}\left(B_s^0 \to \psi(2S)\pi^+\pi^-\right) \times \mathcal{B}\left(\psi(2S) \to J/\psi\pi^+\pi^-\right)} = (6.8 \pm 1.1 \pm 0.2) \times 10^{-2}\,,$$

where the first uncertainty is statistical and the second systematic. The mass spectrum of the $\pi^+\pi^-$ system recoiling against the $\chi_{c1}(3872)$ meson exhibits a large contribution from $B_s^0 \to \chi_{c1}(3872)\,(f_0(980) \to \pi^+\pi^-)$ decays.

1   Introduction

Decays of beauty hadrons to final states with charmonia provide a unique laboratory to study the properties of charmonia and charmonium-like states. A plethora of new states has been observed in such decays, including the $\chi_{c1}(3872)$ particle [1], pentaquark [2–6] and tetraquark [7–18] candidates as well as conventional charmonium states, such as the tensor D-wave $\psi_2(3823)$ meson [19–21]. The nature of many exotic charmonium-like candidates remains unclear. A comparison of their production rates with respect to those of conventional charmonium states in decays of beauty hadrons can shed light on their production mechanisms [22]. For example, the $D^*\overline{D}$ rescattering mechanism [23, 24] would give a large contribution to $\chi_{c1}(3872)$ production and affect the pattern of decay rates of beauty hadrons. There is a puzzling difference between the branching fractions for the $B^+ \to \chi_{c1}(3872)K^+$ and $B^0 \to \chi_{c1}(3872)K^0$ decays [25, 26]. It may be explained by a compact-tetraquark interpretation of the $\chi_{c1}(3872)$ state [27], which simultaneously accounts for the similarity of the branching fractions for the $B^0 \to \chi_{c1}(3872)K^0$ and $B_s^0 \to \chi_{c1}(3872)\phi$ decays [16, 28]. Additional measurements on the $\chi_{c1}(3827)$ production in the decays of beauty hadrons, and in particular, decays of B_s^0 mesons, will be helpful for a better understanding of the nature of the $\chi_{c1}(3872)$ state.

In this paper, the first observation of the $B_s^0 \to \chi_{c1}(3872)\pi^+\pi^-$ decay is reported. This analysis is based on proton-proton (pp) collision data, corresponding to integrated luminosities of 1, 2 and 6 fb^{-1}, collected by the LHCb experiment at centre-of-mass energies of 7, 8 and 13 TeV, respectively. A sample of the $B_s^0 \to J/\psi\pi^+\pi^+\pi^-\pi^-$ decays is used to measure the ratio $\mathcal{R}$ of the branching fractions of the $B_s^0 \to (\chi_{c1}(3872) \to J/\psi\pi^+\pi^-)\,\pi^+\pi^-$ and $B_s^0 \to (\psi(2S) \to J/\psi\pi^+\pi^-)\,\pi^+\pi^-$ decays

$$\mathcal{R} \equiv \frac{\mathcal{B}\left(B_s^0 \to \chi_{c1}(3872)\pi^+\pi^-\right) \times \mathcal{B}\left(\chi_{c1}(3872) \to J/\psi\pi^+\pi^-\right)}{\mathcal{B}\left(B_s^0 \to \psi(2S)\pi^+\pi^-\right) \times \mathcal{B}\left(\psi(2S) \to J/\psi\pi^+\pi^-\right)}\,. \tag{1}$$

The $B_s^0 \to (\chi_{c1}(3872) \to J/\psi\pi^+\pi^-)\,\pi^+\pi^-$ and $B_s^0 \to (\psi(2S) \to J/\psi\pi^+\pi^-)\,\pi^+\pi^-$ decays share the same final state, allowing for a large cancellation of systematic uncertainties.

2   Detector and simulation

The LHCb detector [29, 30] is a single-arm forward spectrometer covering the pseudo-rapidity range $2 < \eta < 5$, designed for the study of particles containing b or c quarks. The detector includes a high-precision tracking system consisting of a silicon-strip vertex detector surrounding the pp interaction region [31], a large-area silicon-strip detector located upstream of a dipole magnet with a bending power of about 4 Tm, and three stations of silicon-strip detectors and straw drift tubes [32, 33] placed downstream of the magnet. The tracking system provides a measurement of the momentum of charged particles with a relative uncertainty that varies from 0.5% at low momentum to 1.0% at 200 GeV/c. The momentum scale is calibrated using samples of $J/\psi \to \mu^+\mu^-$ and $B^+ \to J/\psi K^+$ decays collected concurrently with the data sample used for this analysis [34, 35]. The relative accuracy of this procedure is estimated to be 3×10^{-4} using samples of other fully reconstructed b hadrons, Υ and K_S^0 mesons. The minimum distance of a track to a primary pp-collision vertex (PV), the impact parameter (IP), is measured with a resolution of $(15 + 29/p_T)\,\mu\text{m}$, where p_T is the component of the momentum transverse to the beam,

in GeV/c. Different types of charged hadrons are distinguished using information from two ring-imaging Cherenkov detectors (RICH) [36]. Photons, electrons and hadrons are identified by a calorimeter system consisting of scintillating-pad and preshower detectors, an electromagnetic and a hadronic calorimeter [37]. Muons are identified by a system composed of alternating layers of iron and multiwire proportional chambers [38].

The online event selection is performed by a trigger [39], which consists of a hardware stage, based on information from the calorimeter and muon systems, followed by a software stage, which applies a full event reconstruction. The hardware trigger selects muon candidates with large transverse momentum or dimuon candidates with a large value of the product of the p_T of the muons. In the software trigger, two oppositely charged muons are required to form a good-quality vertex that is significantly displaced from every PV, with a dimuon mass exceeding $2.7\,\text{GeV}/c^2$.

Simulated events are used to describe signal shapes and to compute the efficiencies needed to determine the branching fraction ratios. In the simulation, pp collisions are generated using PYTHIA [40] with a specific LHCb configuration [41]. Decays of unstable particles are described by the EVTGEN package [42], in which final-state radiation is generated using PHOTOS [43]. The interaction of the generated particles with the detector, and its response, are implemented using the GEANT4 toolkit [44] as described in Ref. [45]. The decays $B_s^0 \to \chi_{c1}(3872)\pi^+\pi^-$ and $B_s^0 \to \psi(2S)\pi^+\pi^+$ are simulated using a phase-space decay model that is adjusted to match the mass distributions of the two-pion systems recoiling against the $\chi_{c1}(3827)$ and $\psi(2S)$ mesons in data. In the simulation $\chi_{c1}(3872) \to J/\psi\pi^+\pi^-$ decays proceed via an S-wave $J/\psi\rho^0$ intermediate state [46–48]. The model described in Refs. [49–54] is used for the $\psi(2S) \to J/\psi\pi^+\pi^-$ decays. The simulation is corrected to reproduce the transverse momentum and rapidity distributions of the B_s^0 mesons observed in data. To account for imperfections in the simulation of charged-particle reconstruction, the track reconstruction efficiency determined from simulation is corrected using data-driven techniques [55].

3 Event selection

Candidate $B_s^0 \to J/\psi\pi^+\pi^+\pi^-\pi^-$ decays are reconstructed using the $J/\psi \to \mu^+\mu^-$ decay mode. As explained in detail below, an initial selection criteria similar to those used in Refs. [16,56,57] are used to reduce the background. Subsequently, a multivariate estimator, in the following referred as the MLP classifier, is applied. It is based on an artificial neural network algorithm [58,59] configured with a cross-entropy cost estimator [60].

Muon and hadron candidates are identified using combined information from the RICH, calorimeter and muon detectors [61]. The candidates are required to have a transverse momentum greater than $550\,\text{MeV}/c$ and $200\,\text{MeV}/c$ for muons and pions, respectively. To ensure that the particles can be efficiently separated by the RICH detectors, pions are required to have a momentum between 3.2 and $150\,\text{GeV}/c$. To reduce the combinatorial background due to particles produced promptly in the pp interaction, only tracks that are inconsistent with originating from a PV are used. Pairs of oppositely charged muons consistent with originating from a common vertex are combined to form J/ψ candidates. The mass of the dimuon candidate is required to be between 3.05 and $3.15\,\text{GeV}/c^2$, corresponding to a range of approximately three times the $\mu^+\mu^-$ mass resolution, around the known mass of the J/ψ meson [25]. Selected J/ψ meson candidates are combined with

two pairs of oppositely charged pions to form the $B_s^0 \to J/\psi\pi^+\pi^+\pi^-\pi^-$ candidates and a requirement on the quality of the common six-prong vertex is imposed. To improve the mass and decay time resolution, a kinematic fit [62] is used in which the momentum direction of the B_s^0 candidate is constrained to be collinear to the direction from the PV to the B_s^0 decay vertex, and a mass constraint on the J/ψ state is applied. A requirement on the χ^2 of this fit, χ^2_{fit}, is imposed to reduce the background. The mass of selected $J/\psi\pi^+\pi^+\pi^-\pi^-$ combinations, $m_{J/\psi\pi^+\pi^+\pi^-\pi^-}$, is required to be between 5.30 and 5.48 GeV/c^2. The proper decay time of the B_s^0 candidates is required to be between 0.2 and 2.0 mm/c. The lower limit is used to reduce background from particles coming from the PV while the upper limit suppresses poorly reconstructed candidates. A possible feed down from $\Lambda_b^0 \to J/\psi p\pi^+\pi^-\pi^-$ decays, with the proton misidentified as a pion, is suppressed by rejecting the B_s^0 candidates whose mass, recalculated using the proton hypothesis for one of the pion candidates, is consistent with the known mass of the Λ_b^0 baryon [25].

The final selection of candidates using the MLP classifier is based on the p_{T} and pseudorapidity of J/ψ candidate, the χ^2 of the six-prong vertex, the value of χ^2_{fit}, the proper decay time of the B_s^0 candidates, the transverse momenta of the pions, the dipion mass from the $\chi_{c1}(3872) \to J/\psi\pi^+\pi^-$ decays and the angle between the momenta of the J/ψ and B_s^0 mesons in the $\chi_{c1}(3872)$ rest frame. The MLP classifier is trained on a sample of simulated $B_s^0 \to (\chi_{c1}(3872) \to J/\psi\pi^+\pi^-)\,\pi^+\pi^-$ decays and a background sample of $J/\psi\pi^+\pi^+\pi^-\pi^-$ combinations from the high mass sideband of the B_s^0 signal peak, $5.42 < m_{J/\psi\pi^+\pi^+\pi^-\pi^-} < 5.50$ GeV/c^2. For the background sample, $J/\psi\pi^+\pi^-$ combinations with the $J/\psi\pi^+\pi^-$ mass consistent with the known masses of the $\chi_{c1}(3872)$ state [20,63], $3.86 < m_{J/\psi\pi^+\pi^-} < 3.88$ GeV/c^2, or $\psi(2S)$ meson [25], $3.68 < m_{J/\psi\pi^+\pi^-} < 3.69$ GeV/c^2, are excluded. To avoid introducing a bias in the MLP evaluation, a k-fold cross-validation technique [64] with $k = 7$ is used. The requirement on the MLP classifier is chosen to maximize the Punzi figure of merit $\frac{\varepsilon}{\alpha/2 + \sqrt{B}}$ [65], where ε is the efficiency for the $B_s^0 \to \chi_{c1}(3872)\pi^+\pi^-$ signal, $\alpha = 5$ is the target signal significance and B is the expected background yield. The efficiency ε is estimated using simulation. The expected background yield within the narrow mass window centred around the known masses of the B_s^0 and $\chi_{c1}(3872)$ mesons [25] is determined from fits to data.

The selected B_s^0 candidates with $J/\psi\pi^+\pi^-$ mass within the range $3.85 < m_{J/\psi\pi^+\pi^-} < 3.90$ GeV/c^2 are considered as the $B_s^0 \to \chi_{c1}(3872)\pi^+\pi^-$ candidates. Similarly, the B_s^0 candidates with the $J/\psi\pi^+\pi^-$ mass within the range $3.67 < m_{J/\psi\pi^+\pi^-} < 3.70$ GeV/c^2 are considered as the $B_s^0 \to \psi(2S)\pi^+\pi^-$ candidates. The same MLP classifier is used both for the $B_s^0 \to \chi_{c1}(3872)\pi^+\pi^-$ and $B_s^0 \to \psi(2S)\pi^+\pi^-$ candidates.

4 $B_s^0 \to \chi_{c1}(3872)\pi^+\pi^-$ and $B_s^0 \to \psi(2S)\pi^+\pi^-$ decays

The signal yields for the $B_s^0 \to \chi_{c1}(3872)\pi^+\pi^-$ and $B_s^0 \to \psi(2S)\pi^+\pi^-$ decays are determined using a two-dimensional extended unbinned maximum-likelihood fit to the $J/\psi\pi^+\pi^+\pi^-\pi^-$ and $J/\psi\pi^+\pi^-$ mass distributions. The fit is performed simultaneously in two separate regions of the $J/\psi\pi^+\pi^-$ mass, defined as the $\chi_{c1}(3872)$ region with $3.85 < m_{J/\psi\pi^+\pi^-} < 3.90$ GeV/c^2, and the $\psi(2S)$ region with $3.67 < m_{J/\psi\pi^+\pi^-} < 3.70$ GeV/c^2, which correspond to the $B_s^0 \to \chi_{c1}(3872)\pi^+\pi^-$ and $B_s^0 \to \psi(2S)\pi^+\pi^-$ decays, respectively.

In the $\chi_{c1}(3872)$ region, the two-dimensional fit model is defined as the sum of four

components:

1. A signal component, corresponding to the $B_s^0 \to (\chi_{c1}(3872) \to J/\psi\pi^+\pi^-)\pi^+\pi^-$ decay, described by the product of the B_s^0 and $\chi_{c1}(3872)$ signal templates, discussed in the next paragraph.

2. A component corresponding to $B_s^0 \to J/\psi\pi^+\pi^+\pi^-\pi^-$ decay, where the $J/\psi\pi^+\pi^-$ combination does not originate from a $\chi_{c1}(3872)$ meson, parameterised by the product of the B_s^0 signal template and the phase-space function describing three-body combinations from five-body decays[1] $\Phi_{3,5}(m_{J/\psi\pi^+\pi^-})$ [66], modified by a positive linear polynomial function.

3. A component corresponding to random combinations of the $\chi_{c1}(3872)$ state with a $\pi^+\pi^-$ pair, parameterised as a product of the signal $\chi_{c1}(3872)$ template and a second-order positive-definite polynomial function [67].

4. A component corresponding to random $J/\psi\pi^+\pi^+\pi^-\pi^-$ combinations, parameterized as a two-dimensional non-factorizable positive polynomial function P_{bkg}, that is linear in each variable for a fixed value of the other variable.

In the $\psi(2S)$ region, the two-dimensional fit model is defined in an equivalent way with replacement of the signal $\chi_{c1}(3872)$ template with the signal $\psi(2S)$ template. In this approach we neglect possible interference effects between the first and second components.

The B_s^0 signal shape is modelled with a modified Gaussian function with power-law tails on both sides of the distribution [68,69]. The tail parameters are fixed from simulation, while the mass parameter of the B_s^0 meson is allowed to vary. The detector resolution taken from simulation is corrected by a scale factor, $s_{B_s^0}$, that accounts for a small discrepancy between data and simulation [16,20] and is allowed to vary in the fit.

The $\chi_{c1}(3872)$ and $\psi(2S)$ signal shapes are modelled as relativistic S-wave Breit–Wigner functions convolved with the detector resolution. Due to the proximity of the $\chi_{c1}(3872)$ state to the $D^0\overline{D}^{*0}$ threshold, modelling this component with a Breit–Wigner function may not be adequate [23,70–73]. However, the analyses in Refs. [20,63] demonstrate that a good description of data is obtained with a Breit–Wigner line shape when the detector resolution is included. Mass parameters for the $\chi_{c1}(3872)$ and $\psi(2S)$ signals are allowed to vary in the fit, while the mass difference is constrained to the known value [20]. The width parameters of the $\chi_{c1}(3872)$ and $\psi(2S)$ states are fixed to known values [20,25] using a Gaussian constraint. The detector resolution functions are described by a symmetric modified Gaussian function with power-law tails on both sides of the distribution [68,69], with all parameters determined from simulation. The resolutions are further corrected by a common scale factor, $s_{J/\psi\pi^+\pi^-}$, that accounts for a small discrepancy between data and simulation and is allowed to vary in the fit.

The fit is performed using the B_s^0 mass and the resolution scale factors, $s_{B_s^0}$ and $s_{J/\psi\pi^+\pi^-}$, as shared parameters. The $J/\psi\pi^+\pi^+\pi^-\pi^-$ and $J/\psi\pi^+\pi^-$ mass distributions together with projections of the fit are shown in Fig. 1. The parameters of interest, namely the B_s^0 yields, masses of the B_s^0 meson, $\chi_{c1}(3872)$ and $\psi(2S)$ states, and the resolution scale factors

---

[1]The phase-space mass distribution of a k-body combination of particles from an n-body decay is approximated by $\Phi_{k,n}(x) \propto x_*^{(3k-5)/2}(1-x_*)^{3(n-k)/2-1}$, where $x_* \equiv (x - x_{\min})/(x_{\max} - x_{\min})$, and $x_{\min}, x_{\max}$ denote the minimal and maximal values of x, respectively [66].
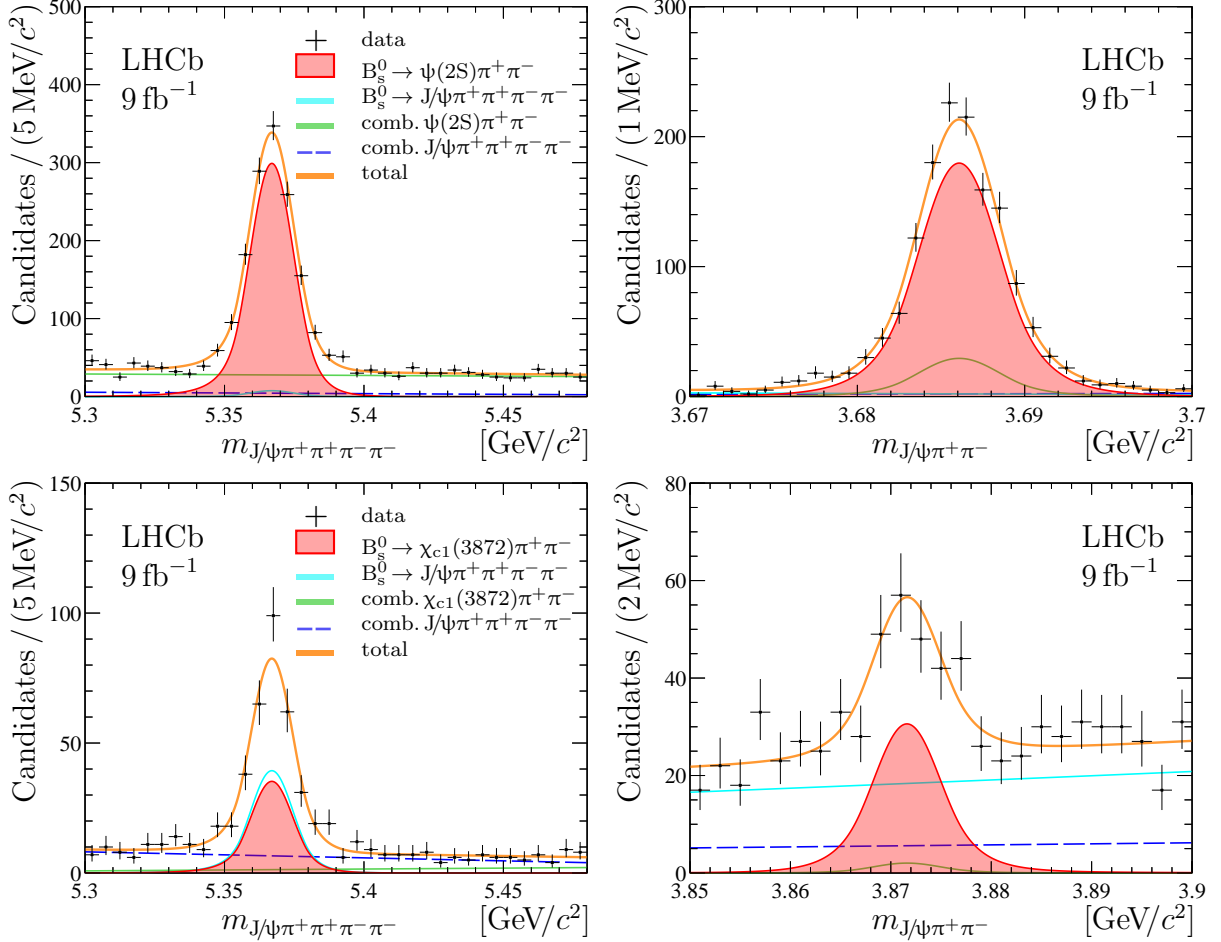
Figure 1: Distributions of the (left) $J/\psi\pi^+\pi^+\pi^-\pi^-$ and (right) $J/\psi\pi^+\pi^-$ mass of selected (top) $B_s^0 \to \psi(2S)\pi^+\pi^-$ and (bottom) $B_s^0 \to \chi_{c1}(3872)\pi^+\pi^-$ candidates. Projections from the fit, described in the text, are overlaid. The $J/\psi\pi^+\pi^+\pi^-\pi^-$ mass distributions are shown for the $B_s^0 \to \psi(2S)\pi^+\pi^-$ and $B_s^0 \to \chi_{c1}(3872)\pi^+\pi^-$ candidates within narrow $J/\psi\pi^+\pi^-$ mass ranges, $3.679 < m_{J/\psi\pi^+\pi^-} < 3.693\,\mathrm{GeV}/c^2$ and $3.864 < m_{J/\psi\pi^+\pi^-} < 3.880\,\mathrm{GeV}/c^2$, respectively. The $J/\psi\pi^+\pi^-$ mass distributions are shown for the B_s^0 candidates within a narrow $J/\psi\pi^+\pi^+\pi^-\pi^-$ mass range, $5.35 < m_{J/\psi\pi^+\pi^+\pi^-\pi^-} < 5.38\,\mathrm{GeV}/c^2$.

are listed in Table 1. The statistical significance for the $B_s^0 \to \chi_{c1}(3872)\pi^+\pi^-$ signal is estimated using Wilks' theorem [74] to be 7.3 standard deviations.

The ratio of branching fractions $\mathcal{R}$, defined in Eq. (1) is calculated as

$$\mathcal{R} = \frac{N_{B_s^0 \to \chi_{c1}(3872)\pi^+\pi^-}}{N_{B_s^0 \to \psi(2S)\pi^+\pi^-}} \times \frac{\varepsilon_{B_s^0 \to \psi(2S)\pi^+\pi^-}}{\varepsilon_{B_s^0 \to \chi_{c1}(3872)\pi^+\pi^-}}, \tag{2}$$

where the signal yields, $N_{B_s^0 \to \chi_{c1}(3872)\pi^+\pi^-}$ and $N_{B_s^0 \to \psi(2S)\pi^+\pi^-}$, are taken from Table 1 and $\varepsilon_{B_s^0 \to \chi_{c1}(3872)\pi^+\pi^-}$ and $\varepsilon_{B_s^0 \to \psi(2S)\pi^+\pi^-}$ are the efficiencies for the $B_s^0 \to \chi_{c1}(3872)\pi^+\pi^-$ and $B_s^0 \to \psi(2S)\pi^+\pi^-$ decays, respectively. The efficiencies are defined as the product of the detector geometric acceptance and the reconstruction, selection, particle identification and trigger efficiencies. All of the efficiency contributions, except the particle identification efficiency, are determined using simulated samples. The efficiencies of the hadron identification are obtained as a function of particle momentum, pseudorapidity and number of

Table 1: Signal yields, hadron masses, and detector resolution scale factors from the simultaneous fit described in the text. The parameters $m_{\mathrm{B_s^0}}$, $s_{\mathrm{B_s^0}}$ and $s_{\mathrm{J/\psi\pi^+\pi^-}}$ are shared in the fit among the two mass ranges. The uncertainties are statistical only.

Parameter		$\mathrm{B_s^0} \to \chi_{\mathrm{c1}}(3872)\pi^+\pi^-$	$\mathrm{B_s^0} \to \psi(2S)\pi^+\pi^-$
N		155 ± 23	1301 ± 47
$m_{\chi_{c1}(3872)}$	[MeV/c^2]	3871.57 ± 0.09	—
$m_{\psi(2S)}$	[MeV/c^2]	—	3686.08 ± 0.07
$m_{\mathrm{B_s^0}}$	[MeV/c^2]	5366.97 ± 0.23	
$s_{\mathrm{B_s^0}}$		1.06 ± 0.03	
$s_{\mathrm{J/\psi\pi^+\pi^-}}$		1.12 ± 0.03	

charged tracks in the event using dedicated calibration samples of $\mathrm{D}^{*+} \to (\mathrm{D}^0 \to \mathrm{K}^-\pi^+)\,\pi^+$ and $\mathrm{K_S^0} \to \pi^+\pi^-$ decays selected in data [36, 75]. The efficiency ratio is found to be

$$\frac{\varepsilon_{\mathrm{B_s^0}\to\psi(2S)\pi^+\pi^-}}{\varepsilon_{\mathrm{B_s^0}\to\chi_{c1}(3872)\pi^+\pi^-}} = 0.57 \pm 0.01 \,,$$

where the uncertainty is due to the limited size of the simulated samples. The efficiency ratio differs from unity due to the different p_{T} spectra of pions in the $\psi(2S) \to \mathrm{J/\psi}\pi^+\pi^-$ and the $\chi_{\mathrm{c1}}(3872) \to \mathrm{J/\psi}\pi^+\pi^-$ decays. The resulting value of $\mathcal{R}$ is

$$\mathcal{R} = (6.8 \pm 1.1) \times 10^{-2} \,, \tag{3}$$

where the uncertainty is statistical.

5 Dipion mass spectrum

The mass spectra for the dipion system recoiling against the $\chi_{\mathrm{c1}}(3872)$ and $\psi(2S)$ states are obtained using the *sPlot* technique [76], based on results of the two-dimensional fit described in previous section. The spectra shown in Fig. 2 exhibit significant deviations from the phase-space distribution and are similar to the $\pi^+\pi^-$ mass spectrum observed in the $\mathrm{B_s^0} \to \mathrm{J/\psi}\pi^+\pi^-$ decay [77–79] and the S-wave $\pi^+\pi^-$ component in $\mathrm{D_s^+} \to \pi^+\pi^+\pi^-$ decays [80, 81].

In Ref. [77] it has been found that the $\pi^+\pi^-$ mass spectrum from $\mathrm{B_s^0} \to \mathrm{J/\psi}\pi^+\pi^-$ decays can be described by a coherent sum of the $\mathrm{f_0}(980)$ amplitude and a contribution from a high-mass scalar meson, initially identified as the $\mathrm{f_0}(1370)$ state. References [82, 83] suggest a better interpretation of the high-mass state as the $\mathrm{f_0}(1500)$ resonance. A dedicated amplitude analysis from Ref. [79] followed this suggestion and confirmed the dominant $\mathrm{f_0}(980)$ and $\mathrm{f_0}(1500)$ contributions in $\mathrm{B_s^0} \to \mathrm{J/\psi}\pi^+\pi^-$ decays. Assuming a similarity with the $\mathrm{B_s^0} \to \mathrm{J/\psi}\pi^+\pi^-$ decays, the mass spectra of the dipion system recoiling against the $\chi_{\mathrm{c1}}(3872)$ and $\psi(2S)$ states are described with a function consisting of two components:

- A component corresponding to a coherent sum of the scalar $\mathrm{f_0}(980)$ and $\mathrm{f_0}(1500)$ amplitudes and parameterised as

$$F(m) \propto mqp^3 \left| f\mathcal{A}_{\mathrm{f_0}(980)}(m) + \mathrm{e}^{i\varphi}\mathcal{A}_{\mathrm{f_0}(1500)}(m) \right|^2 \,, \tag{4}$$
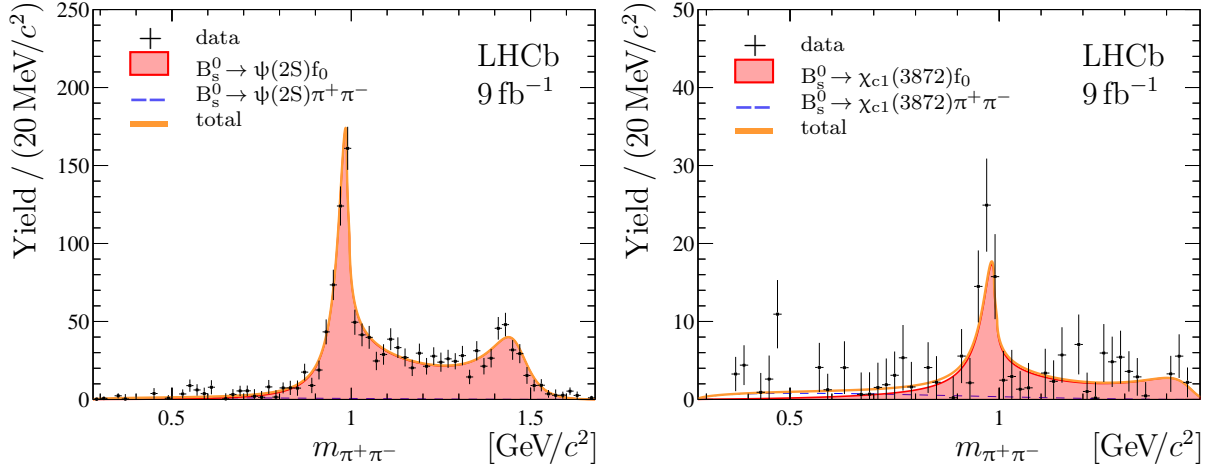
6

Figure 2: The background-subtracted mass spectra for the dipion system recoiling against the $\chi_{c1}(3872)$ or $\psi(2S)$ states for (left) $B_s^0 \to \psi(2S)\pi^+\pi^-$ and (right) $B_s^0 \to \chi_{c1}(3872)\pi^+\pi^-$ decays. The results of the fit, described in the text, are overlaid.

where m is the $\pi^+\pi^-$ mass, q is the momentum of the π^+ meson in the $\pi^+\pi^-$ rest frame, p is the momentum of the $\pi^+\pi^-$ system in the B_s^0 rest frame, $\mathcal{A}_{f_0(980)}$ and $\mathcal{A}_{f_0(1500)}$ are the $f_0(980)$ and $f_0(1500)$ amplitudes, φ is a relative phase and the real coefficient f characterises the relative contributions of the $f_0(980)$ and $f_0(1500)$ components. The amplitude $\mathcal{A}_{f_0(1500)}$ is parameterised as a relativistic S-wave Breit–Wigner function, while the modified Flatté–Bugg amplitude [84, 85] (see Eq. (18) in Ref. [79]) is used for the $f_0(980)$ state.

- A component corresponding to incoherent nonresonant contribution and parameterised by the $\Phi_{2,3}(m)$ phase-space function.

The fit is performed simultaneously for the dipion mass spectra from the $B_s^0 \to \chi_{c1}(3872)\pi^+\pi^+$ and $B_s^0 \to \psi(2S)\pi^+\pi^+$ decays. The shape parameters of the $f_0(980)$ and $f_0(1500)$ states are shared in the fit. To stabilise the fit, Gaussian constraints are applied to the parameters of the $f_0(980)$ state and the mass and width of the $f_0(1500)$ state, according to Solution I from Ref. [79].

The fit results are shown in Fig. 2. This simplistic model qualitatively describes the major contributions to the dipion mass spectrum from $B_s^0 \to \psi(2S)\pi^+\pi^-$ decays and supports the hypothesis of the dominant contribution of two S-wave resonances. The fit indicates the necessity of a dedicated analysis to properly account for the sub-leading contributions. The same model, consisting of two coherent contributions from the $f_0(980)$ and $f_0(1500)$ states describes well the dipion mass spectrum from the $B_s^0 \to \chi_{c1}(3872)\pi^+\pi^-$ decay. The statistical significance for the $B_s^0 \to \chi_{c1}(3872)f_0(980)$ decay is estimated using Wilks' theorem and found to be 9.1 standard deviations.

6 Systematic uncertainties

Due to the similar decay topologies, systematic uncertainties largely cancel in the ratio $\mathcal{R}$. The remaining contributions to systematic uncertainties are summarized in Table 2 and discussed below.

The systematic uncertainties arising from imperfect knowledge of the signal and background shapes used for determination of the $B_s^0 \to \chi_{c1}(3872)\pi^+\pi^-$ and $B_s^0 \to \psi(2S)\pi^+\pi^-$ signal yields are estimated with alternative models. For the B_s^0 signal shape the bifurcated Student's t-distribution [86], Apollonios and Hypatia distributions [87] are tested as alternative models. The $J/\psi\pi^+\pi^-$ mass resolution functions are also modelled with Student's t-distribution and symmetric Apollonios functions. For the Breit–Wigner functions describing the $\chi_{c1}(3872)$ and $\psi(2S)$ signal shapes, the natural widths are varied within the known uncertainties [20, 25, 63]. The degree of the polynomial functions used for the parameterisation of the background and the non-resonant $J/\psi\pi^+\pi^-$ components is varied by one unit. Exponential functions are used as components in alternative background models. In addition, the detector resolution scale factors $s_{B_s^0}$ and $s_{J/\psi\pi^+\pi^-}$ are constrained to values of $s_{B_s^0} = 1.04 \pm 0.02$, $s_{J/\psi\pi^+\pi^-} = 1.06 \pm 0.02$ from Ref. [16] and $s_{B_s^0} = 1.052 \pm 0.003$, $s_{J/\psi\pi^+\pi^-} = 1.048 \pm 0.004$ from Ref. [20] using Gaussian constraints. For each alternative model the ratio of the $B_s^0 \to \chi_{c1}(3872)\pi^+\pi^-$ and $B_s^0 \to \psi(2S)\pi^+\pi^-$ signal yields is recalculated. The maximum relative deviation with respect to the baseline value is found to be 2.5% which is assigned as a relative systematic uncertainty for the ratio $\mathcal{R}$. The fit procedure itself is tested using a large sample of pseudoexperiments, generated using the default model with parameters extracted from data and the results are found to be unbiased.

The $B_s^0 \to \chi_{c1}(3872)\pi^+\pi^-$ and $B_s^0 \to \psi(2S)\pi^+\pi^-$ decays are simulated as phase-space decays and corrected to reproduce the dipion mass spectra observed in data. A weighting procedure, based on a gradient boosted tree algorithm [88], is used for corrections of simulated samples. The systematic uncertainty related to the correction method is estimated by varying the hyper-parameters of the regression trees ensemble. The maximum deviation from the baseline value, 0.9%, is taken as the uncertainty associated with the unknown B_s^0 decay models.

An additional systematic uncertainty on the ratios arises due to differences between data and simulation. In particular, there are differences in the reconstruction efficiency of charged-particle tracks that do not cancel completely in the ratio due to the different kinematic distributions of the final-state particles. The track-finding efficiencies obtained from simulated samples are corrected using data-driven techniques [55]. The uncertainties related to the efficiency correction factors, together with the uncertainty on

Table 2: Relative systematic uncertainties (in %) for the ratio of branching fractions. The sources are described in the text.

Source	$\sigma_{\mathcal{R}}$ [%]
Fit model	2.5
B_s^0 decay model	0.9
Efficiency corrections	0.1
Trigger efficiency	1.1
Data-simulation difference	2.0
Simulated sample size	0.5
Sum in quadrature	3.5

the hadron-identification efficiency due to the finite size of the calibration samples [36, 75], are propagated to the ratios of the total efficiencies using pseudoexperiments and amount to 0.1%.

A systematic uncertainty on the ratios related to the knowledge of the trigger efficiencies is estimated by comparing the ratios of trigger efficiencies in data and simulation for large samples of $B^+ \to J/\psi K^+$ and $B^+ \to \psi(2S)K^+$ decays [89] and is taken to be 1.1% for all three ratios of branching fractions.

Remaining data-simulation differences, that are not previously discussed, are investigated by varying the selection criteria. The resulting variations in the ratios of the efficiency-corrected yields do not exceed 2%, which is taken as the corresponding systematic uncertainty. The final systematic uncertainty considered on the ratios of branching fractions is due to the knowledge of the ratios of efficiencies in Eq. (2), limited by the size of simulated samples. It is determined to be 0.5%.

No systematic uncertainty is included for the admixture of the CP-odd and CP-even B_s^0 eigenstates in the $B_s^0 \to \chi_{c1}(3872)\pi^+\pi^-$ and $B_s^0 \to \psi(2S)\pi^+\pi^-$ decays [90], which is assumed to be the same for both channels. Analysis of the dipion spectrum from the $B_s^0 \to \psi(2S)\pi^+\pi^-$ decays in Sec. 5 indicates that the final state is predominantly CP-odd, with the effective lifetime corresponding to the heavy-mass long-lifetime B_s^0 eigenstate [91–93]. The dipion spectrum from the $B_s^0 \to \chi_{c1}(3872)\pi^+\pi^-$ decays is also consistent with being predominantly CP-odd. In the extreme case that the $B_s^0 \to \chi_{c1}(3872)\pi^+\pi^-$ decay is an equal mixture of the short-lifetime and long-lifetime eigenstates, the corresponding ratio of branching fractions would change by 2.4 %.

The statistical significance for the $B_s^0 \to \chi_{c1}(3872)\pi^+\pi^-$ decay is recalculated using Wilks' theorem for each alternative fit model, and the smallest value of 7.3 standard deviations is taken as the significance that includes the systematic uncertainty.

Alternative models are used also for the fit to the dipion mass spectra from the $B_s^0 \to \chi_{c1}(3872)\pi^+\pi^-$ and $B_s^0 \to \psi(2S)\pi^+\pi^-$ channels. In particular, Solution II from Ref. [79] is investigated as an alternative external constraint for the $f_0(980)$ and $f_0(1500)$ parameters. The model with the $f_0(1370)$ resonance instead of the $f_0(1500)$ state is used as alternative model with a constraint to the known parameters of the $f_0(1370)$ state [25]. As an alternative model for the noncoherent nonresonant component, a product of the $\Phi_{2,3}$ phase-space function and the positive second-order polynomial function [67] has been probed. Also, a coherent nonresonant contribution, parameterised with a complex-valued constant function, is added to the function from Eq. (4). The smallest significance for the $B_s^0 \to \chi_{c1}(3872)f_0(980)$ decay is found to be 7.4 standard deviations, which is taken as the significance including systematic uncertainty.

7 Summary

An observation of the $B_s^0 \to \chi_{c1}(3872)\pi^+\pi^-$ decays with significance exceeding 7 standard deviations is reported using proton-proton collision data, corresponding to integrated luminosities of 1, 2 and 6 fb^{-1}, collected by the LHCb experiment at centre-of-mass energies of 7, 8 and 13 TeV, respectively. Using the $B_s^0 \to \psi(2S)\pi^+\pi^-$ decay as a normalization channel, and neglecting the possible interference effects, the ratio of branching fractions is

measured to be

$$\frac{\mathcal{B}\left(B_s^0 \to \chi_{c1}(3872)\pi^+\pi^-\right) \times \mathcal{B}\left(\chi_{c1}(3872) \to J/\psi\pi^+\pi^-\right)}{\mathcal{B}\left(B_s^0 \to \psi(2S)\pi^+\pi^-\right) \times \mathcal{B}\left(\psi(2S) \to J/\psi\pi^+\pi^-\right)} = (6.8 \pm 1.1 \pm 0.2) \times 10^{-2},$$

where the first uncertainty is statistical and the second systematic. The measured ratio of the branching fractions exceeds by a factor of three the analogous ratio for the $B_s^0 \to \chi_{c1}(3872)\phi$ and $B_s^0 \to \psi(2S)\phi$ decays reported in Refs. [16, 28]. Using the known branching fractions for the $B_s^0 \to \psi(2S)\pi^+\pi^-$, and $\psi(2S) \to J/\psi\pi^+\pi^-$ decays [25], the branching fraction for the $B_s^0 \to (\chi_{c1}(3872) \to J/\psi\pi^+\pi^-)\pi^+\pi^-$ is calculated to be

$$\mathcal{B}\left(B_s^0 \to \chi_{c1}(3872)\pi^+\pi^-\right) \times \mathcal{B}\left(\chi_{c1}(3872) \to J/\psi\pi^+\pi^-\right) = (1.6 \pm 0.3 \pm 0.1 \pm 0.3) \times 10^{-6},$$

where the third uncertainty is due to imprecise knowledge of the branching fractions for the $B_s^0 \to \psi(2S)\pi^+\pi^-$ and $\psi(2S) \to J/\psi\pi^+\pi^-$ decays [25].

The mass spectrum of the dipion system recoiling against the $\chi_{c1}(3872)$ state shows a similarity with those from the $B_s^0 \to \psi(2S)\pi^+\pi^-$ and $B_s^0 \to J/\psi\pi^+\pi^-$ decays [79], compatible with a dominant S-wave contribution, and exhibits a large $B_s^0 \to \chi_{c1}(3872)f_0(980)$ component with significance exceeding 7 standard deviations. With a larger data sample and better understanding of the S-wave $\pi^+\pi^-$ scattering [94], a precise determination of the $f_0(980)$ component in this decay will be possible.

References

[1] Belle collaboration, S. K. Choi *et al.*, *Observation of a narrow charmoniumlike state in exclusive* $B^{\pm} \to K^{\pm}\pi^{+}\pi^{-}J/\psi$ *decays*, Phys. Rev. Lett. **91** (2003) 262001, `arXiv:hep-ex/0309032`.

[2] LHCb collaboration, R. Aaij *et al.*, *Observation of* $J/\psi p$ *resonances consistent with pentaquark states in* $\Lambda_{b}^{0} \to J/\psi p K^{-}$ *decays*, Phys. Rev. Lett. **115** (2015) 072001, `arXiv:1507.03414`.

[3] LHCb collaboration, R. Aaij *et al.*, *Model-independent evidence for* $J/\psi p$ *contributions to* $\Lambda_{b}^{0} \to J/\psi p K^{-}$ *decays*, Phys. Rev. Lett. **117** (2016) 082002, `arXiv:1604.05708`.

[4] LHCb collaboration, R. Aaij *et al.*, *Observation of a narrow pentaquark state,* $P_{c}(4312)^{+}$, *and of two-peak structure of the* $P_{c}(4450)^{+}$, Phys. Rev. Lett. **122** (2019) 222001, `arXiv:1904.03947`.

[5] LHCb collaboration, R. Aaij *et al.*, *Evidence for exotic hadron contributions to* $\Lambda_{b}^{0} \to J/\psi p \pi^{-}$ *decays*, Phys. Rev. Lett. **117** (2016) 082003, `arXiv:1606.06999`.

[6] LHCb collaboration, R. Aaij *et al.*, *Evidence of a* $J/\psi\Lambda$ *structure and observation of excited* Ξ^{-} *states in the* $\Xi_{b}^{-} \to J/\psi\Lambda K^{-}$ *decay*, Science Bulletin **66** (2021) 1278, `arXiv:2012.10380`.

[7] Belle collaborationn, S. K. Choi *et al.*, *Observation of a resonance-like structure in the* $\pi^{\pm}\psi'$ *mass distribution in exclusive* $B \to K\pi^{\pm}\psi'$ *decays*, Phys. Rev. Lett. **100** (2008) 142001, `arXiv:0708.1790`.

[8] Belle collaboration, R. Mizuk *et al.*, *Dalitz analysis of* $B \to K\pi^{+}\psi'$ *decays and the* $Z(4430)^{+}$, Phys. Rev. **D80** (2009) 031104, `arXiv:0905.2869`.

[9] Belle collaboration, K. Chilikin *et al.*, *Experimental constraints on the spin and parity of the* $Z(4430)^{+}$, Phys. Rev. **D88** (2013) 074026, `arXiv:1306.4894`.

[10] LHCb collaboration, R. Aaij *et al.*, *Observation of the resonant character of the* $Z(4430)^{-}$ *state*, Phys. Rev. Lett. **112** (2014) 222002, `arXiv:1404.1903`.

[11] LHCb collaboration, R. Aaij *et al.*, *Model-independent confirmation of the* $Z(4430)^{-}$ *state*, Phys. Rev. **D92** (2015) 112009, `arXiv:1510.01951`.

[12] LHCb collaboration, R. Aaij *et al.*, *Observation of exotic* $J/\psi\phi$ *structures from amplitude analysis of* $B^{+} \to J/\psi\phi K^{+}$ *decays*, Phys. Rev. Lett. **118** (2017) 022003, `arXiv:1606.07895`.

[13] LHCb collaboration, R. Aaij *et al.*, *Amplitude analysis of* $B^{+} \to J/\psi\phi K^{+}$ *decays*, Phys. Rev. **D95** (2017) 012002, `arXiv:1606.07898`.

[14] LHCb collaboration, R. Aaij *et al.*, *Evidence for an* $\eta_{c}(1S)\pi^{-}$ *resonance in* $B^{0} \to \eta_{c}(1S)K^{+}\pi^{-}$ *decays*, Eur. Phys. J. **C78** (2018) 1019, `arXiv:1809.07416`.

[15] LHCb collaboration, R. Aaij *et al.*, *Model-independent observation of exotic contributions to* $B^0 \to J/\psi K^+ \pi^-$ *decays*, Phys. Rev. Lett. **122** (2019) 152002, arXiv:1901.05745.

[16] LHCb collaboration, R. Aaij *et al.*, *Study of* $B_s^0 \to J/\psi \pi^+ \pi^- K^+ K^-$ *decays*, JHEP **02** (2021) 024, arXiv:2011.01867.

[17] LHCb collaboration, R. Aaij *et al.*, *Observation of new resonances decaying to* $J/\psi K^+$ *and* $J/\psi \phi$, Phys. Rev. Lett. **127** (2021) 082001, arXiv:2103.01803.

[18] LHCb collaboration, R. Aaij *et al.*, *Evidence for a new structure in the* $J/\psi p$ *and* $J/\psi \overline{p}$ *systems in* $B_s^0 \to J/\psi p \overline{p}$ *decays*, Phys. Rev. Lett. **128** (2022) 062001, arXiv:2108.04720.

[19] Belle collaboration, V. Bhardwaj *et al.*, *Evidence of a new narrow resonance decaying to* $\chi_{c1}\gamma$ *in* $B \to \chi_{c1}\gamma K$, Phys. Rev. Lett. **111** (2013) 032001, arXiv:1304.3975.

[20] LHCb collaboration, R. Aaij *et al.*, *Study of the* $\psi_2(3823)$ *and* $\chi_{c1}(3872)$ *states in* $B^+ \to (J/\psi \pi^+ \pi^-) K^+$ *decays*, JHEP **08** (2020) 123, arXiv:2005.13422.

[21] LHCb collaboration, R. Aaij *et al.*, *Study of charmonium and charmonium-like contributions in* $B^+ \to J/\psi \eta K^+$ *decays*, JHEP **04** (2021) 46, arXiv:2202.04045.

[22] L. Maiani, A. D. Polosa, and V. Riquer, *A theory of* X *and* Z *multiquark resonances*, Phys. Lett. **B778** (2018) 247, arXiv:1712.05296.

[23] P. Artoisenet, E. Braaten, and D. Kang, *Using line shapes to discriminate between binding mechanisms for the* X(3872), Phys. Rev. **D82** (2010) 014013, arXiv:1005.2167.

[24] E. Braaten, L.-P. He, and K. Ingles, *Production of* X(3872) *accompanied by a pion in* B *meson decay*, Phys. Rev. **D100** (2019) 074028, arXiv:1902.03259.

[25] Particle Data Group, R. L. Workman *et al.*, *Review of particle physics*, Prog. Theor. Exp. Phys. **2022** (2022) 083C01.

[26] Belle collaboration, H. Hirata *et al.*, *Study of the lineshape of* X(3872) *using* B *decays to* $D^0 \overline{D}^{*0} K$, arXiv:2302.02127.

[27] L. Maiani, A. D. Polosa, and V. Riquer, *The* X(3872) *tetraquarks in* B *and* B_s *decays*, Phys. Rev. **D102** (2020) 034017, arXiv:2005.08764.

[28] CMS collaboration, A. M. Sirunyan *et al.*, *Observation of the* $B_s^0 \to X(3872)\phi$ *decay*, Phys. Rev. Lett. **125** (2020) 152001, arXiv:2005.04764.

[29] LHCb collaboration, A. A. Alves Jr. *et al.*, *The LHCb detector at the LHC*, JINST **3** (2008) S08005.

[30] LHCb collaboration, R. Aaij *et al.*, *LHCb detector performance*, Int. J. Mod. Phys. **A30** (2015) 1530022, arXiv:1412.6352.

[31] R. Aaij *et al.*, *Performance of the LHCb Vertex Locator*, JINST **9** (2014) P09007, arXiv:1405.7808.

[32] R. Arink *et al.*, *Performance of the LHCb Outer Tracker*, JINST **9** (2014) P01002, `arXiv:1311.3893`.

[33] P. d'Argent *et al.*, *Improved performance of the LHCb Outer Tracker in LHC Run 2*, JINST **12** (2017) P11016, `arXiv:1708.00819`.

[34] LHCb collaboration, R. Aaij *et al.*, *Measurements of the Λ_b^0, Ξ_b^-, and Ω_b^- baryon masses*, Phys. Rev. Lett. **110** (2013) 182001, `arXiv:1302.1072`.

[35] LHCb collaboration, R. Aaij *et al.*, *Precision measurement of D meson mass differences*, JHEP **06** (2013) 065, `arXiv:1304.6865`.

[36] M. Adinolfi *et al.*, *Performance of the LHCb RICH detector at the LHC*, Eur. Phys. J. **C73** (2013) 2431, `arXiv:1211.6759`.

[37] C. Abellan Beteta *et al.*, *Calibration and performance of the LHCb calorimeters in Run 1 and 2 at the LHC*, `arXiv:2008.11556`, submitted to JINST.

[38] A. A. Alves Jr. *et al.*, *Performance of the LHCb muon system*, JINST **8** (2013) P02022, `arXiv:1211.1346`.

[39] R. Aaij *et al.*, *The LHCb trigger and its performance in 2011*, JINST **8** (2013) P04022, `arXiv:1211.3055`.

[40] T. Sjöstrand, S. Mrenna, and P. Skands, *A brief introduction to* Pythia 8.1, Comput. Phys. Commun. **178** (2008) 852, `arXiv:0710.3820`.

[41] I. Belyaev *et al.*, *Handling of the generation of primary events in* Gauss*, the LHCb simulation framework*, J. Phys. Conf. Ser. **331** (2011) 032047.

[42] D. J. Lange, *The* EvtGen *particle decay simulation package*, Nucl. Instrum. Meth. **A462** (2001) 152.

[43] P. Golonka and Z. Was, Photos *Monte Carlo: A precision tool for QED corrections in Z and W decays*, Eur. Phys. J. **C45** (2006) 97, `arXiv:hep-ph/0506026`.

[44] Geant4 collaboration, J. Allison *et al.*, Geant4 *developments and applications*, IEEE Trans. Nucl. Sci. **53** (2006) 270; Geant4 collaboration, S. Agostinelli *et al.*, Geant4*: A simulation toolkit*, Nucl. Instrum. Meth. **A506** (2003) 250.

[45] M. Clemencic *et al.*, *The LHCb simulation application,* Gauss*: Design, evolution and experience*, J. Phys. Conf. Ser. **331** (2011) 032023.

[46] LHCb collaboration, R. Aaij *et al.*, *Determination of the X(3872) meson quantum numbers*, Phys. Rev. Lett. **110** (2013) 222001, `arXiv:1302.6269`.

[47] LHCb collaboration, R. Aaij *et al.*, *Quantum numbers of the X(3872) state and orbital angular momentum in its $\rho^0 J/\psi$ decays*, Phys. Rev. **D92** (2015) 011102(R), `arXiv:1504.06339`.

[48] LHCb collaboration, R. Aaij *et al.*, *Observation of sizeable ω contribution to $\chi_{c1} \to \pi^+\pi^- J/\psi$ decays*, `arXiv:2204.12597`, to appear in Phys. Rev. D.

[49] K. Gottfried, *Hadronic transitions between quark-antiquark bound states*, Phys. Rev. Lett. **40** (1978) 598.

[50] M. B. Voloshin, *On dynamics of heavy quarks in non-perturbative QCD vacuum*, Nucl. Phys. **B154** (1979) 365.

[51] M. E. Peskin, *Short-distance analysis for heavy-quark systems: (I). Diagrammatics*, Nucl. Phys. **B156** (1979) 365.

[52] G. Bhanot and M. E. Peskin, *Short-distance analysis for heavy-quark systems: (II). Applications*, Nucl. Phys. **B156** (1979) 391.

[53] M. B. Voloshin and V. I. Zakharov, *Measuring QCD anomalies in hadronic transitions between onium states*, Phys. Rev. Lett. **45** (1980) 688.

[54] V. A. Novikov and M. A. Shifman, *Comment on the $\psi' \to J/\psi\pi\pi$ decay*, Z. Phys. **C8** (1981) 43.

[55] LHCb collaboration, R. Aaij *et al.*, *Measurement of the track reconstruction efficiency at LHCb*, JINST **10** (2015) P02007, `arXiv:1408.1251`.

[56] LHCb collaboration, R. Aaij *et al.*, *Observation of $\Lambda_b^0 \to \psi(2S)pK^-$ and $\Lambda_b^0 \to J/\psi\pi^+\pi^-pK^-$ decays and a measurement of the Λ_b^0 baryon mass*, JHEP **05** (2016) 132, `arXiv:1603.06961`.

[57] LHCb collaboration, R. Aaij *et al.*, *Observation of the $\Lambda_b^0 \to \chi_{c1}(3872)pK^-$ decay*, JHEP **09** (2019) 028, `arXiv:1907.00954`.

[58] W. S. McCulloch and W. Pitts, *A logical calculus of the ideas immanent in nervous activity*, The bulletin of mathematical biophysics **5** (1943) 115.

[59] F. Rosenblatt, *The perceptron: A probabilistic model for information storage and organization in the brain*, Psychological Review **65** (1958) 386.

[60] J.-H. Zhong *et al.*, *A program for the Bayesian neural network in the* ROOT *framework*, Comput. Phys. Commun. **182** (2011) 2655, `arXiv:1103.2854`.

[61] A. Powell *et al.*, *Particle identification at LHCb*, PoS **ICHEP2010** (2010) 020, LHCb-PROC-2011-008.

[62] W. D. Hulsbergen, *Decay chain fitting with a Kalman filter*, Nucl. Instrum. Meth. **A552** (2005) 566, `arXiv:physics/0503191`.

[63] LHCb collaboration, R. Aaij *et al.*, *Study of the line shape of the $\chi_{c1}(3872)$ state*, Phys. Rev. **D102** (2020) 092005, `arXiv:2005.13419`.

[64] S. Geisser, *Predictive inference: An introduction*, Chapman and Hall/CRC, New York, 1993.

[65] G. Punzi, *Sensitivity of searches for new signals and its optimization*, eConf **C030908** (2003) MODT002, `arXiv:physics/0308063`.

[66] E. Byckling and K. Kajantie, *Particle kinematics*, John Wiley & Sons Inc., New York, 1973.

[67] S. Karlin and L. S. Shapley, *Geometry of moment spaces*, vol. 12 of *Memoirs of the American Mathematical Society*, American Mathematical Society, Providence, Rhode Island, 1953.

[68] LHCb collaboration, R. Aaij *et al.*, *Observation of J/ψ-pair production in* pp *collisions at* $\sqrt{s} = 7\,TeV$, Phys. Lett. **B707** (2012) 52, arXiv:1109.0963.

[69] T. Skwarnicki, *A study of the radiative cascade transitions between the* Υ' *and* Υ *resonances*, PhD thesis, Institute of Nuclear Physics, Krakow, 1986, DESY-F31-86-02.

[70] C. Hanhart, Y. S. Kalashnikova, A. E. Kudryavtsev, and A. V. Nefediev, *Reconciling the* X(3872) *with the near-threshold enhancement in the* $D^0\overline{D}^{*0}$ *final state*, Phys. Rev. **D76** (2007) 034007, arXiv:0704.0605.

[71] E. Braaten and J. Stapleton, *Analysis of* J/ψπ⁺π⁻ *and* $D^0\overline{D}^0\pi^0$ *decays of the* X(3872), Phys. Rev. **D81** (2010) 014019, arXiv:0907.3167.

[72] Y. S. Kalashnikova and A. V. Nefediev, *Nature of* X(3872) *from data*, Phys. Rev. **D80** (2009) 074004, arXiv:0907.4901.

[73] C. Hanhart, Y. S. Kalashnikova, and A. V. Nefediev, *Interplay of quark and meson degrees of freedom in a near-threshold resonance: multi-channel case*, Eur. Phys. J. **A47** (2011) 101, arXiv:1106.1185.

[74] S. S. Wilks, *The large-sample distribution of the likelihood ratio for testing composite hypotheses*, Ann. Math. Stat. **9** (1938) 60.

[75] R. Aaij *et al.*, *Selection and processing of calibration samples to measure the particle identification performance of the LHCb experiment in Run 2*, Eur. Phys. J. Tech. Instr. **6** (2019) 1, arXiv:1803.00824.

[76] M. Pivk and F. R. Le Diberder, *sPlot: A statistical tool to unfold data distributions*, Nucl. Instrum. Meth. **A555** (2005) 356, arXiv:physics/0402083.

[77] LHCb collaboration, R. Aaij *et al.*, *First observation of* $B_s^0 \to$ J/ψf₀(980) *decays*, Phys. Lett. **B698** (2011) 115, arXiv:1102.0206.

[78] LHCb collaboration, R. Aaij *et al.*, *Measurement of the CP violating phase* ϕ_s *in* $\overline{B}_s^0 \to$ J/ψf₀(980), Phys. Lett. **B707** (2012) 497, arXiv:1112.3056.

[79] LHCb collaboration, R. Aaij *et al.*, *Measurement of resonant and CP components in* $\overline{B}_s^0 \to$ J/ψπ⁺π⁻ *decays*, Phys. Rev. **D89** (2014) 092006, arXiv:1402.6248.

[80] BES III collaboration, M. Ablikim *et al.*, *Amplitude analysis of the* $D_s^+ \to \pi^+\pi^-\pi^+$ *decay*, Phys. Rev. **D106** (2022) 112006, arXiv:2108.10050.

[81] LHCb collaboration, R. Aaij *et al.*, *Amplitude analysis of the* $D_s^+ \to \pi^-\pi^+\pi^+$ *decay*, arXiv:2209.09840, to appear in JHEP.

[82] W. Ochs, *Spectroscopy with glueballs and the role of* $f_0(1370)$, Acta Phys. Polon. Supp. **6** (2013) 839, arXiv:1304.7634.

[83] W. Ochs, *The status of glueballs*, J. Phys. **G40** (2013) 043001, arXiv:1301.5183.

[84] S. M. Flatté, *Coupled-channel analysis of the* $\pi\eta$ *and* $K\overline{K}$ *systems near* $K\overline{K}$ *threshold*, Phys. Lett. **B63** (1976) 224.

[85] D. V. Bugg, *Re-analysis of data on* $a_0(1450)$ *and* $a_0(980)$, Phys. Rev. **D78** (2008) 074023, arXiv:0808.2706.

[86] Student (W. S. Gosset), *The probable error of a mean*, Biometrika **6** (1908) 1.

[87] D. Martínez Santos and F. Dupertuis, *Mass distributions marginalized over per-event errors*, Nucl. Instrum. Meth. **A764** (2014) 150, arXiv:1312.5000.

[88] A. Rogozhnikov, *Reweighting with boosted decision trees*, J. Phys. Conf. Ser. **762** (2016) 012036, arXiv:1608.05806.

[89] LHCb collaboration, R. Aaij *et al.*, *Measurement of relative branching fractions of B decays to* $\psi(2S)$ *and* J/ψ *mesons*, Eur. Phys. J. **C72** (2012) 2118, arXiv:1205.0918.

[90] K. De Bruyn *et al.*, *Branching ratio measurements of* B_s^0 *decays*, Phys. Rev. **D86** (2012) 014027, arXiv:1204.1735.

[91] LHCb collaboration, R. Aaij *et al.*, *Measurement of the* $\overline{B}_s^0$ *effective lifetime in the* $J/\psi f_0(980)$ *final state*, Phys. Rev. Lett. **109** (2012) 152002, arXiv:1207.0878.

[92] D0 collaboration, V. M. Abazov *et al.*, B_s^0 *lifetime measurement in the CP-odd decay channel* $B_s^0 \to J/\psi f_0(980)$, Phys. Rev. **D94** (2016) 012001, arXiv:1603.01302.

[93] CMS collaboration, A. M. Sirunyan *et al.*, *Measurement of b-hadron lifetimes in* pp *collisions at* $\sqrt{s} = 8$ *TeV*, Eur. Phys. J. **C78** (2018) 457, Erratum ibid. **C78** (2018) 562, arXiv:1710.08949.

[94] S. Ropertz, C. Hanhart, and B. Kubis, *A new parametrization for the scalar pion form factors*, Eur. Phys. J. **C78** (2018) 1000, arXiv:1809.06867.